Compact Wide-Angle Scanning Multibeam Antenna Array for V2X Communications

Muhammad Kamran Ishfaq, Suleiman Aliyu Babale, Hassan Tariq Chattha, Mohamed Himdi, Ali Raza, Muhammad Younas, Tharek ABD. Rahman, Sharul Kamal Abdul Rahim, *Member, IEEE*, and Bilal A. Khawaja

***Abstract*—This letter presents a wide-angle scanning multibeam planar inverted-E antenna (PIEA) array for vehicle-to-everything communication. The compact four-element PIEA array is designed with 0.3λ_o spacing, which achieves 90° wide-angle scanning when a 135° phase shift is applied obtained using a 4 × 4 Butler matrix (BM). The closeness of the array elements causes high mutual coupling and high cross polarization at wider scan angles. Therefore, three novel techniques are employed to overcome the high cross polarization and mutual coupling between the antenna elements in this array. To feed the antenna array, a low-cost miniaturized beamforming 4 × 4 BM circuit is designed without the use of phase shifters and conventional crossovers. The total dimensions of the compact PIEA array are just 0.456λ_0 × 1.12λ_0 × 0.036λ_0, while the overall dimensions of the multibeam array, including BM, are 2.731λ_0 × 2.2λ_0 × 0.046 λ_0. This multibeam array achieves for the first time the wide-angle scanning angles of ±87° with a 3 dB beam scanning range of ±120° along with the scanning angles of ±20°. This array design can be scaled to use as an antenna array for millimeter-wave applications.**

***Index Terms*—Butler matrix (BM), modified coupler, mutual coupling, phase shifter, planar inverted-E antenna (PIEA) array, vehicle-to-everything (V2X), wide-angle scanning.**

Manuscript received May 2, 2021; revised June 20, 2021; accepted July 12, 2021. Date of publication July 27, 2021; date of current version November 16, 2021. This work was supported in part by the Deanship of Scientific Research, Islamic University of Madinah, under Grant 16/40; in part by the Tertiary Education Trust Fund, Nigeria; in part by Universiti Teknologi Malaysia; and in part by the Institute of Electronics and Telecommunications of Rennes, University of Rennes I, France. *(Corresponding author: Muhammad Kamran Ishfaq.)*

Muhammad Kamran Ishfaq and Ali Raza are with the Department of Electrical Engineering and Technology, Government College University Faisalabad, Faisalabad 38000, Pakistan (e-mail: kamranzarrar@gmail.com; raza015@gmail.com).

Muhammad Younas is with the Department of Computer Science, Government College University Faisalabad, Faisalabad 38000, Pakistan (e-mail: younas.76@gmail.com).

Suleiman Aliyu Babale is with the Department of Electrical Engineering, Bayero University, Kano 700241, Nigeria (e-mail: sababale.ele@buk.edu.ng).

Hassan Tariq Chattha and Bilal A. Khawaja are with the Department of Electrical Engineering, Faculty of Engineering, Islamic University of Madinah, Madinah 41411, Saudi Arabia (e-mail: chattha43@hotmail.com; bam.khawaja@gmail.com).

Mohamed Himdi is with the Institut d'Electronique et des Technologies du numéRique, UMR CNRS 6164, University of Rennes I, 35042 Rennes, France (e-mail: mohamed.himdi@univ-rennes1.fr).

Tharek ABD. Rahman and Sharul Kamal Abdul Rahim are with the Wireless Communication Center, University Teknologi Malaysia, Johor Bahru 80140, Malaysia (e-mail: tharek@utm.my; sharulkamal@fke.utm.my).

Digital Object Identifier 10.1109/LAWP.2021.3100349

I. Introduction

THE driverless cars and the autonomous driving features in vehicles have greatly increased the interest in the vehicle-to-everything (V2X) communications (see Fig. 1). At present, V2X communication is relying on dedicated short-range communication (DSRC) 5.9 GHz (5.85–5.925 GHz) band [1], [2]. In the future, cellular-V2X communication will make use of readily available 5G infrastructure at sub 6-GHz, 28 GHz, and 39 GHz bands [3]. To bring V2X to fruition, wide coverage antennas, multiple-input-multiple-output (MIMO), compact switched beam arrays, and beamforming arrays are the key enabling antenna technologies [3], [4]. The switch beamforming network (SBFN), which is an arrangement of the antenna array, capable of generating a highly directive beam and steer it to desired directions [5]. There are several types of SBFN, such as the Blass matrix [6], the Rotman lens [7], the Nolen matrix [8], and the Butler matrix (BM) [9]. The most popular among these techniques is BM for having a relatively simple configuration and low-power dissipations [10]–[13].

For designing compact arrays, mutual coupling severely degrades the performance of the beamforming arrays [14]. The research works in [14] and [17] presented compact designs but had a limited scanning range using high-cost phase shifters. The design in [15] is a compact phased array using high-cost phase shifters, but it had limited scanning and very high cross polarization around 0 dB at 70° scan angle, making it unable to be used for wide-angle scanning. The research in [16] presented a wide-angle scanning array using reconfigurable pattern elements with a scanning range of ±75°. However, the design is not compact (spacing, 1.2λ).

This letter presents a low-cost, miniaturized compact multibeam wide-angle scanning array at DSRC 5.9 GHz band for V2X communication. Since compact arrays suffer from high mutual coupling [14] and high cross polarization at wider scan angles [15], therefore, to mitigate mutual coupling and high cross polarization, three novel techniques are employed, which include employing a reduced-size planar inverted-E antenna (PIEA), etching long slots in between adjacent array elements, and designing and placing two decoupling meandered line (ML) structures in between the adjacent array elements. To feed the antenna array, a miniaturized BM is designed without the use of phase shifters and classical crossovers. Hence, for the first time, the far beam is achieved at ±87° using the novel compact angle scanning multibeam PIEA array proposed with 0.3λ_o spacing.

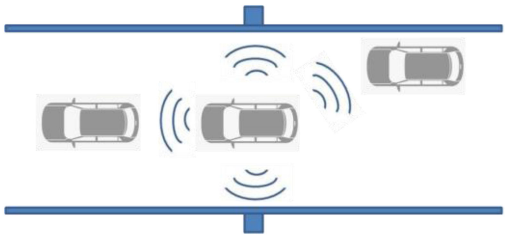

Fig. 1. Vehicle-to-vehicle communication example.

The array design can also be scaled to millimeter wave, as presented in [18].

II. Wide-Angle Scanning Array Design

A PIEA array is designed with a $0.3\lambda_0$ spacing to achieve wide-angle scanning. Using PIEA (a modified dual shorting PIFA) as an array element results in reduced mutual coupling due to the formation of a naturally formed slot antenna in between the neighboring array elements [19]. However, it suffers from high cross polarization and poor gain at wider scanning angles [15]. Thus, to overcome high cross polarization and high mutual coupling, the following design procedure/techniques are employed.

1) As a first step, the single PIEA is designed with the compact structure having reduced width to accommodate the increased intercorner spacing S_e while maintaining spacing to $0.3\lambda_{0.}$ It helps in reducing radiations due to the naturally formed slot antenna in between the two adjacent antenna elements.
2) To reduce mutual coupling, the slots having width S_e are etched in the ground plane in between each of the two adjacent array elements. It reduces the coupling current between the two adjacent antennas.
3) To further reduce mutual coupling and cross polarization, two decoupling ML structures possessing high inductive reactance are introduced at distances Y_{S2} and Y_{C2} from the PIEA corner, in the slots in between each of the two adjacent array elements, as shown in Fig. 2(c). The ML-structure detailed dimensions are zoomed-in in Fig. 2(c).

To feed the antenna array using BM, a feeding mechanism is designed. All the array elements are fed by a 50 Ω microstrip feedline ($L_{f2} \times W_{f2}$), etched at L_{f1}, as shown in Fig. 2(b). The copper of the feed-side ground blocks the slots and decoupling ML structure. To avoid blockage and any variation in the impedance of ML structures, all the forms of copper are etched except which is precisely below the feedline [i.e., $L_{f2} \times W_{f2}$, as shown in Fig. 2(c)].

Fig. 2 shows the three-dimensional (3-D) and back view of the proposed compact antenna array having four PIEA elements. Fig. 2(a) shows the configuration of a single element. Roger RT/Duroid 3003 ($\epsilon_r = 3$) is used as the dielectric material (thickness, $t = 0.25$ mm). Table I lists the optimized values of the design parameters of the array.

The S_{11} and $S_{22} < -10$ dB, as shown in Fig. 3(a), indicate that the array is performing well from 5.3 to 6.75 GHz. The

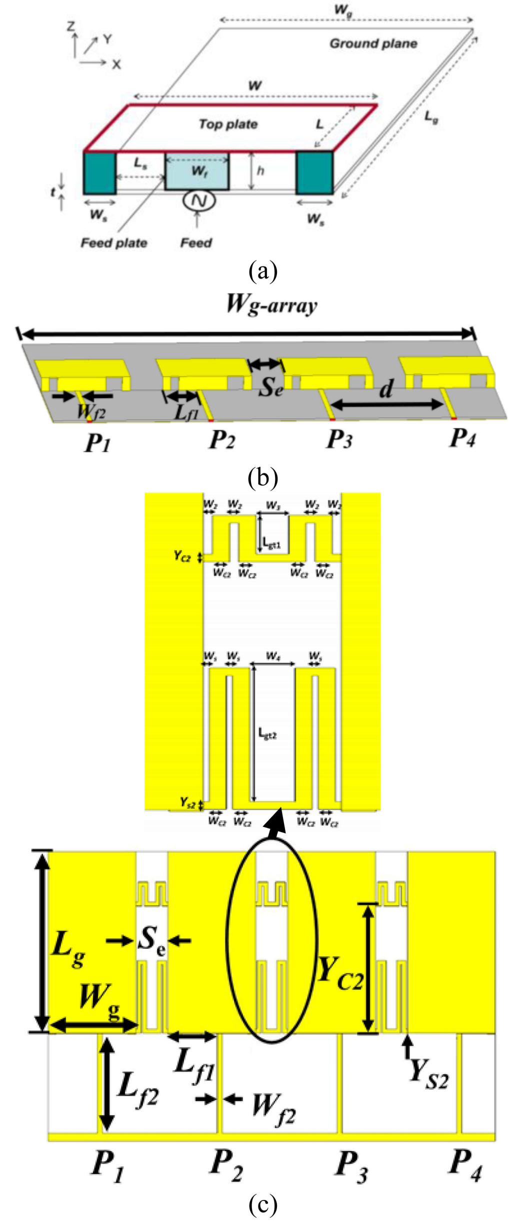

Fig. 2. PIEA array. (a) Single element. (b) Array top with the feeding part. (c) Array ground plane with zoomed-in, highlighting the decoupling structure.

TABLE I
Optimized Design Values of PIEA Array

Parameter	Value (mm)	Parameter	Value (mm)
W_{c2}	0.5	L_{f1}	2.5
$W=W_G$	11	d_e	15
L_G	22.8	Se	4
W_S	1	L_{f2}	12.5
W_f	6	L_{gt1}	2.5
L	8.5	L_{gt2}	8.61
h	1.8	W_2	0.26
L_S	1	W_3	0.95
W_{f2}	0.615	W_4	1.31
Y_{C2}	16	W_5	0.15
Y_{S2}	0.04	t	0.25
Wg_array	56	λ_0 (5.9 GHz)	50.8

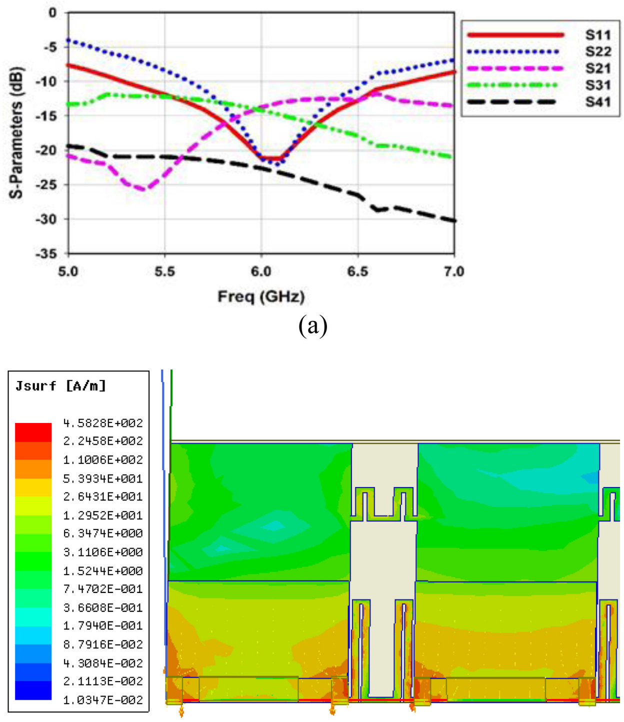

(a)

(b)

Fig. 3. PIEA array. (a) *S*-parameters (dB). (b) Current distribution.

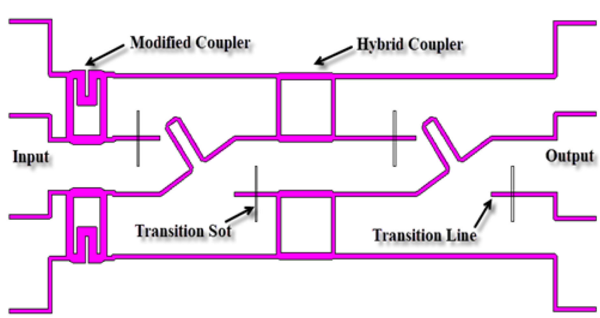

Fig. 4. Layout of the cross-coupled BM.

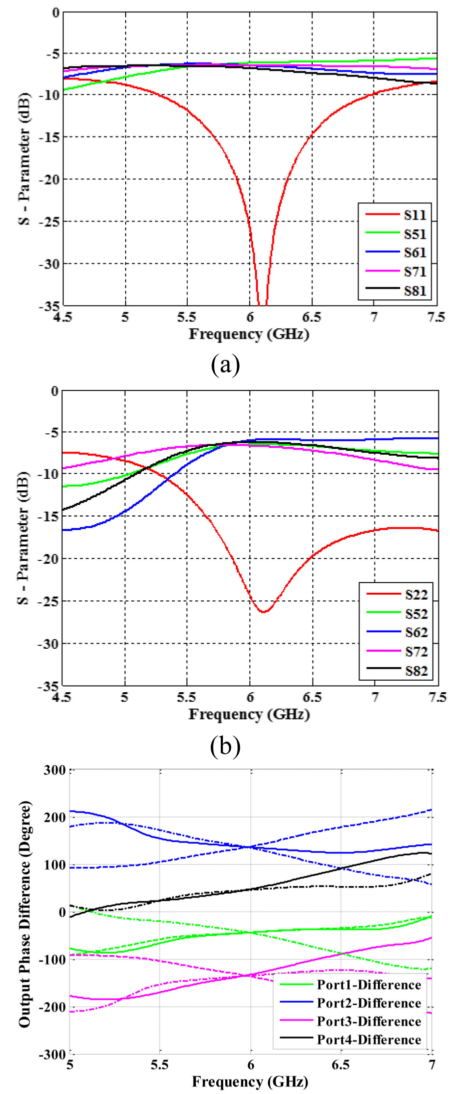

(a)

(b)

(c)

Fig. 5. Reflection and transmission coefficients when (a) ports 1 and 3 are excited and (b) ports 2 and 4 are excited. (c) Output phase differences (P1–P4).

mutual couplings S_{12} and $S_{23} < -10$ dB show that the techniques employed have effectively suppressed the mutual coupling. The current distribution, as shown in Fig. 3(b), shows that the decoupling ML structure exhibits a high inductance, which reduces the mutual coupling. The opposite current flowing in the ML structure cancels out the radiations, which helps to minimize the cross polarization.

III. BM Design

Generally, 4 × 4 BM consists of 90° couplers, 45° phase shifters, and crossovers by combining two 90° couplers [10]. In this letter, the BM without phase shifters is designed using the cross-coupled crossover. The 4 × 4 BM presented in this letter utilizes only the microstrip couplers and a crossover in a planar structure. Employing the modified 45° couplers in this design eliminates the use of phase shifters [20]. This reduces the dimension and transmission loss of the device by shortening the transmission line path, thus reducing the problem of insertion loss and reducing the number of components required in forming BM. The layout of the BM is shown in Fig. 4.

Fig. 5(a) shows the reflection coefficient and transmission coefficients when port 1 of the BM is energized. Likewise, Fig. 5(b) shows the *S*-parameters when port 2 of the BM is energized, while the remaining three ports are terminated with a 50 Ω load. Similarly, due to the symmetry of the BM, exciting ports 3 and 4 has a similar effect as ports 2 and 1, respectively. From Fig. 5(c), it can also be seen that the progressive phase differences at the outputs of the BM are +45°, −135°, +135°, and −45° at the operating frequency, when ports 1, 2, 3, and 4 are excited, respectively. This conforms with the theoretical values.

IV. Fabrication and Measurements

The proposed multibeam wide-angle scanning PIEA array design was excited using the 4 × 4 BM designed in Section III,

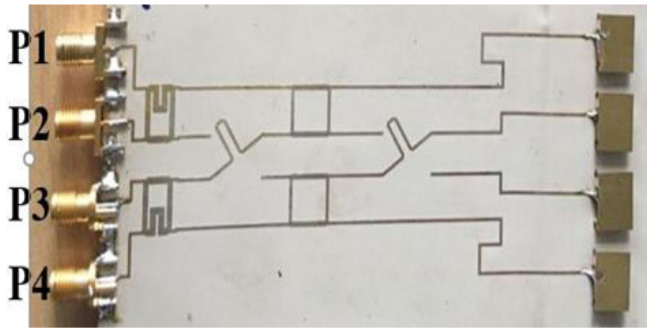

Fig. 6. Photograph of the multibeam antenna array.

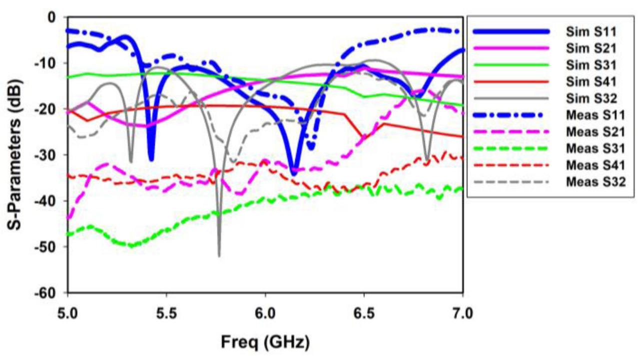

Fig. 7. *S*-parameters of the multibeam array.

TABLE II
SIMULATED AND MEASURED BEAM POSITIONS

Port No.		P1	P2	P3	P4
Beam Position(θ^0)	Simulated	+87°	-20°	+20°	-87°
	Measured	+86°	-20°	+20°	-86°
3 dB Beamwidth		71°	45.8°	44.4°	79.2°

and the overall system was tested and measured in an anechoic chamber. Fig. 6 shows the complete fabricated prototype of the multibeam antenna array. Fig. 7 shows the simulated and measured *S*-parameters of the compact multibeam PIEA array when Port 1 is fed. Between 5.5 and 6.3 GHz, the reflection coefficients and port isolations are below < -10 dB, which confirms that the multibeam array performs well for DSRC 5.9 GHz band. When ports 2 and 3 of the BM are excited, the main pattern radiates at an angle of $\pm 20°$ with a cross polarization < -18 dB, and when the power is excited at ports 1 and 4, the angle switches to $\pm 87°$ with a cross polarization < -13 dB. The output radiation patterns are depicted in Fig. 8. Both the measurements and the simulation results matched with little disparity due to fabrication limitations. Most of the 4×4 BM multibeam array literature shows the multibeam at $\pm 14°$ and $\pm 48°$ [9], [10] while this design radiates multibeam at $\pm 20°$ and $\pm 87°$. The reason for this wide scanning angle using 4×4 BM is because of the closeness of the array spacing to $0.3\lambda_0$, achieved by employing the novel techniques to effectively reduce mutual coupling and cross polarization.

Hence, a very wide-angle maximum azimuthal scanning angle of $\pm 87°$ with a 3 dB scanning range of $\pm 120°$ is achieved using a compact miniaturized multibeam array. Table II lists the simulated and measured beam positions of each beam.

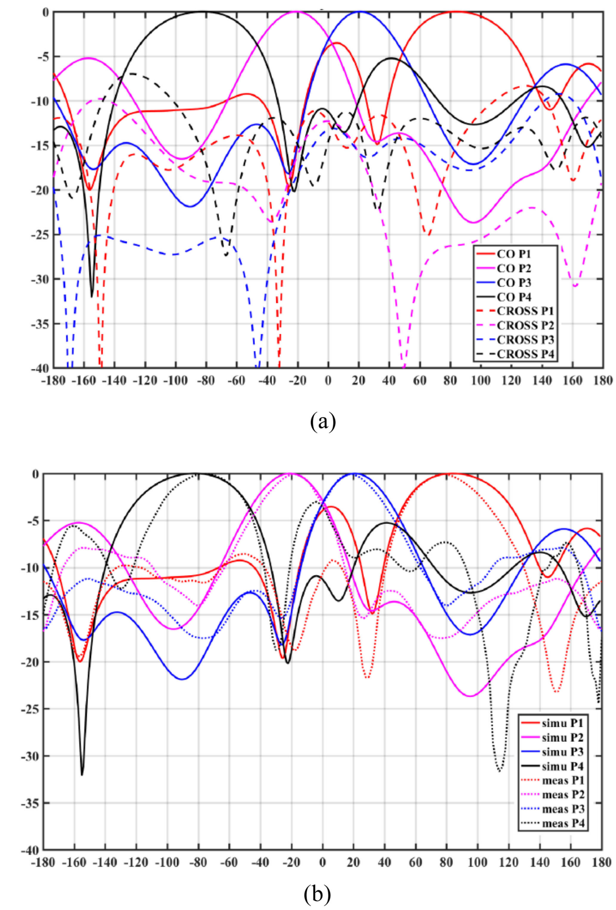

Fig. 8. Multibeam capability (*H*-plane). (a) Simulated. (b) Measured.

V. CONCLUSION

This letter has presented a novel miniaturized compact multibeam wide-angle scanning PIEA array with a spacing of 0.3λ, designed, fabricated, and characterized for the V2X applications. As a reduced array, interelement spacing results in high mutual coupling and cross polarization. Therefore, to suppress mutual coupling and high cross polarization, the design employs novel techniques that are a compact PIEA designed with reduced width to accommodate an increased intercorner spacing, the slots etched in between the adjacent array elements, and two decoupling meandered line high impedance structures in these slots. This proposed PIEA array design is fed by a compact miniaturized 4×4 BM. BM is designed without using phase shifters and conventional crossover. A slot-couple line is designed as a substitution of classical crossovers. With these techniques, when the compact multibeam array is developed, the far beams were successfully achieved, for the first time at $\pm 87°$, with a 3 dB beam scanning range of $\pm 120°$. Multibeam array produced four beams at $-87°$, $-20°$, $+20°$, and $+87°$. The wide-angle scanning array design can be used as a phased array by using phase shifters to achieve a continuous 3 dB scanning range of 240° ($\pm 120°$) and can be scaled to millimeter wave.

REFERENCES

[1] L. Huang and Y. Lu, "A switchable or MIMO antenna for V2X communication," in *Proc. IEEE Int. Conf. Comput. Electromagn.*, 2019, pp. 1–2.

[2] S. Chen *et al.*, "Vehicle-to-everything (V2X) services supported by LTE-based systems and 5G," *IEEE Commun. Standards Mag.*, vol. 1, no. 2, pp. 70–76, 2017.

[3] A. Nasr, K. Sarabandi, and M. Takla, "Multi-beam dual-polarized windshield antenna with wide elevation coverage for 5G V2X applications," in *Proc. IEEE Int. Symp. Antennas Propag. North Amer. Radio Sci. Meeting*, 2020, pp. 1333–1334.

[4] V. Rabinovich and N. Alexandrov, *Antenna Arrays and Automotive Applications*. New York, NY, USA: Springer, 2013.

[5] T. Djerafi and K. Wu, "A low-cost wideband 77-GHz planar Butler matrix in SIW technology," *IEEE Trans. Antennas Propag.*, vol. 60, no. 10, pp. 4949–4954, Oct. 2012.

[6] C. Tsokos *et al.*, "Analysis of a multibeam optical beamforming network based on Blass matrix architecture," *J. Lightw. Technol.*, vol. 36, no. 16, pp. 3354–3372, Aug. 2018.

[7] Y. Gao, M. Khaliel, F. Zheng, and T. Kaiser, "Rotman lens based hybrid analog-digital beamforming in massive MIMO systems: Array architectures, beam selection algorithms and experiments," *IEEE Trans. Veh. Technol.*, vol. 66, no. 10, pp. 9134–9148, Oct. 2017.

[8] N. J. G. Fonseca and N. Ferrando, "Nolen matrix with tapered amplitude law for linear arrays with reduced side lobe level," in *Proc. 4th Eur. Conf. Antennas Propag.*, 2010, pp. 1–5.

[9] S. Aliyubabale, S. H. Lawan, S. K. A. Rahim, and S. Ifeomaorakwue, "Implementation of 4×4 Butler matrix using silver-nono instant inkjet printing technology," in *Proc. IEEE 3rd Int. Conf. Electro-Technol. Nat. Develop.*, 2017, pp. 514–518.

[10] Q.-L. Yang, Y.-L. Ban, K. Kang, C.-Y.-D. Sim, and G. Wu, "SIW multibeam array for 5G mobile devices," *IEEE Access*, vol. 4, pp. 2788–2796, 2016.

[11] C. Bartlett and J. Bornemann, "Cross-configuration substrate integrated waveguide beamforming network for 1D and 2D beam patterns," *IEEE Access*, vol. 7, pp. 151827–151835, 2019.

[12] S. A. Babale *et al.*, "Miniaturized Butler matrix beamforming network using 3dB non-standard couplers," *Zaria J. Elect. Eng. Technol.*, vol. 9, no. 2, pp. 11–15, 2020.

[13] S. I. Orakwue, R. Ngah, O. Elija, and S. A. Babale, "Cascaded Butler matrix with two-dimensional beam scanning capability at 28 GHz for 5G wireless system," *Adv. Sci. Lett.*, vol. 24, pp. 3937–3939, 2018.

[14] J. Nasir, M. H. Jamaluddin, M. R. Kamarudin, I. Ullah, Y.-C. Lo, and R. Selvaraju, "A four-element linear dielectric resonator antenna array for beamforming applications with compensation of mutual coupling," *IEEE Access*, vol. 4, pp. 6427–6437, 2016.

[15] M. K. Ishfaq *et al.*, "Compact four-element phased antenna array for 5G applications," *IEEE Access*, vol. 7, pp. 161103–161111, 2019.

[16] X. Ding, B.-Z. Wang, and G.-Q. He, "Research on a millimeter-wave phased array with wide-angle scanning performance," *IEEE Trans. Antennas Propag.*, vol. 61, no. 10, pp. 5319–5324, Oct. 2013.

[17] Y. Wang, L. Zhu, H. Wang, Y. Luo, and G. Yang, "A compact, scanning tightly coupled dipole array with parasitic strips for next-generation wireless applications," *IEEE Antennas Wireless Propag. Lett.*, vol. 17, no. 4, pp. 534–537, Apr. 2018.

[18] M. Kamran Ishfaq, T. Abdul Rahman, H. T. Chattha, and M. Khalily, "A novel millimeter wave linear PIFA array antenna for 5G next generation wireless communication system," in *Proc. 1st Int. Conf. Innov. Sci. Technol.*, Apr. 2015, pp. 664–668.

[19] S. Zhang, S. N. Khan, and S. He, "Reducing mutual coupling for an extremely closely-packed tunable dual-element PIFA array through a resonant slot antenna formed in between," *IEEE Trans. Antennas Propag.*, vol. 58, no. 8, pp. 2771–2776, Aug. 2010.

[20] S. A. Babale, S. K. Abdul Rahim, O. A. Barro, M. Himdi, and M. Khalily, "Single layered 4×4 Butler matrix without phase-shifters and crossovers," *IEEE Access,* vol. 6, pp. 77289–77298, 2018.